The life, death, and ROMP activity of ruthenium complexes containing the basic, chelating diphosphine bis(dicyclohexyl)-1,4-phosphinobutane

Dino Amoroso, Glenn P.A. Yap, and Deryn E. Fogg

Abstract: Reaction of $RuCl_2(PPh_3)_3$ with bis(dicyclohexyl)-1,4-phosphinobutane (dcypb) under N_2 affords access to a formerly elusive family of dcypb complexes based on the $RuCl_2(PP)$ core. Under Ar or vacuum atmosphere, decomposition occurs via Ru-promoted dehydrogenation of the dcypb ligand. While the N_2-stabilized species $[RuCl_2(dcypb)]_2(N_2)$ (**4a**) is easily handled under N_2 in nonchlorinated solvents, reaction with chlorinated solvents rapidly yields paramagnetic $Ru_2Cl_5(dcypb)_2$ (**5**). The N_2 ligand within **4a** is readily displaced under H_2 or CO atmosphere, yielding $Ru_2Cl_4(dcypb)_2(H_2)$ (**6**) or $RuCl_2(dcypb)(CO)_2$, the latter as a mixture of *ccc*-(**7**) and *tcc*-(**8**) isomers. Benzylidene derivative $RuCl_2(dcypb)(CHPh)$ (**1a**), prepared in situ by reaction of **4a** with $PhCHN_2$, proves exceptionally active in ring-opening metathesis polymerization (ROMP) of norbornene. The X-ray crystal structure of **5** is reported: triclinic, a = 13.390(2), b = 15.726(2), c = 19.524(2) Å, α = 77.325(2), β = 70.964(2), γ = 73.478(2)°, with space group $P\bar{1}$ and Z = 2.

Key words: ruthenium, alkylphosphine, dehydrogenation, carbene, metathesis, crystal structure.

Résumé : La réaction du $RuCl_2(PPh_3)_3$ avec le bis(dicyclohexyl)-1,4-phosphinobutane (dcypb), sous atmosphère d'azote, permet d'accéder à la famille antérieurement élusive de complexes de dcypb comportant un noyau $RuCl_2(PP)$. Sous atmosphère d'argon ou sous vide, il se produit une décomposition qui se produit par le biais d'une déshydrogénation du ligand dcypb provoquée par le Ru. Alors que l'on peut facilement manipuler l'espèce stabilisée par le N_2 $[RuCl_2(dcypb)]_2(N_2)$, **4a**, sous atmosphère d'azote, dans des solvants non chlorés, la réaction dans des solvants chlorés conduit à la formation de l'espèce paramagnétique $Ru_2Cl_5(dcypb)_2$, **5**. On peut facilement déplacer le ligand N_2 du composé **4a** sous atmosphère de H_2 ou de CO avec formation de $Ru_2Cl_4(dcypb)_2(H_2)$, **6**, ou de $RuCl_2(dcypb)(CO)_2$ qui existe sous la forme de mélange d'isomères *ccc*-(**7**) et *tcc*-(**8**). Le dérivé benzylidène, $RuCl_2(dcypb)(CHPh)$, **1a**, préparé in situ par réaction du composé **4a** avec $PhCHN_2$, est exceptionnellement actif dans la polymérisation par ouverture de cycle et métathèse du norbornène. On a déterminé la structure cristalline par diffraction des rayons X du composé **5**: triclinique, a = 13,390(2), b = 15,726(2) et c = 19,524(2)Å, α = 77,325(2), β = 70,964(2) et γ = 73,478(2)°, groupe d'espèce $P\bar{1}$ et Z = 2.

Mots clés : ruthénium, alkylphosphine, déshydrogénation, carbène, métathèse, structure cristalline.

[Traduit par la Rédaction]

Introduction

Enhanced catalytic activity is associated with use of electron-rich phosphine ligands in a range of reactions promoted by late transition metal complexes, including metathesis (1, 2) and hydrogenation (3, 4) catalysis. Complexes of chelating alkyldiphosphines remain little explored in such chemistry, relative to the ubiquitous aryldiphosphine derivatives. We recently described the first Ru–diphosphine catalysts to exhibit high activity in ring-opening metathesis polymerization (ROMP) without ligand loss (2). Benzylidene catalysts $RuCl_2(PP)(CHPh)$ (PP = $R_2P(CH_2)_4PR_2$; R = Cy (dcypb, 1,4-bis(dicyclohexylphosphino)butane) (**1a**), R = Ph (dppb, 1,4-bis(diphenylphosphino)butane) (**1b**)) were generated in situ by reaction of mixed-phosphine species $RuCl_2(PP)(PPh_3)$ (**2**) or dimeric $[RuCl_2(dppb)]_2$ with phenyldiazomethane. The inhibiting effect of free PPh_3 was explored within the $RuCl_2(dppb)(PPh_3)$–$[RuCl_2(dppb)]_2$ pair, but no route to the corresponding $[RuCl_2(dcypb)]_2$ precursor existed. Here we report a new route to PPh_3-free Ru complexes containing the chelating, basic diphosphine ligand dcypb, with insights into decomposition pathways that have until now hindered the broader deployment of such systems. The ROMP activity of the PPh_3-free system is described.

Received September 5, 2000. Published on the NRC Research Press Web site at http://canjchem.nrc.ca on July 11, 2001.

Dedicated to Professor Brian R. James on the occasion of his retirement, in honour of his outstanding contributions to catalysis and chemistry.

D. Amoroso, G.P.A. Yap, and D.E. Fogg.[1] Center for Catalysis Innovation and Research, Department of Chemistry, University of Ottawa, Ottawa, ON K1N 6N5, Canada.

[1]Corresponding author (telephone: (613) 562-5800 ext. 6057; fax: (613) 562-5170; e-mail: dfogg@science.uottawa.ca).

Experimental

Unless otherwise stated, all operations were performed under N_2 using standard Schlenk or drybox techniques. Dry, oxygen-free solvents were obtained using an Anhydrous Engineering solvent purification system, and stored over Linde 4 Å molecular sieves. $CDCl_3$ and C_6D_6 were dried over activated sieves (Linde 4 Å) and degassed by consecutive

 DOI: 10.1139/cjc-79-5/6-958

freeze-pump-thaw cycles. Phenyldiazomethane (5), dcypb (6), $RuCl_2(PPh_3)_3$ (**3**) (7), and *t*-$RuCl_2(dppe)_2$ (8) were prepared according to literature procedures. $RuCl_3 \cdot 3H_2O$ was purchased from Strem Chemicals. Norbornene was purchased from Aldrich and distilled from sodium under N_2. Hydrogen (Praxair, UHP grade) was passed through a Deoxo cartridge and Drierite column in series; CO (Praxair) was used as received.

^{31}P and ^{13}C NMR spectra were recorded on a Varian XL-300 spectrometer, ^1H NMR spectra on a Varian Gemini 200 or Bruker AMX-500 spectrometer. Peaks are reported in ppm, relative to 85% aq. H_3PO_4 (^{31}P) or the deuterated solvent (^1H, ^{13}C). Solid state NMR data were recorded on a Bruker ASX-200 MHz spectrometer, infrared spectra on a Bomem MB100 IR spectrometer. Microanalytical data were obtained using a PerkinElmer Series II CHNS/O instrument. Gel permeation chromatography (GPC) data were obtained with CH_2Cl_2 as eluent (flow rate 1.0 mL min^{-1}; samples 1–2 mg mL^{-1}) using a Wyatt DAWN light-scattering instrument equipped with Optilab DSP refractometer, HPLC system with a Waters model 515 pump, Rheodyne model 7725i injector with a 200 μL injection loop, and Waters Styragel HR3 column.

Preparation of $Ru_2Cl_4(dcypb)_2(N_2)$ (4a)

A green solution of **3** (500 mg, 0.52 mmol) and dcypb (259 mg, 0.57 mmol) in C_6H_6 (5 mL) was stirred at 21°C under N_2. Orange **4a** began to precipitate from solution within 1 h. The orange suspension was diluted with hexanes after 18 h and the product was filtered off, washed with hexanes (3 × 10 mL), and dried under a steady flow of N_2 for 24 h. Yield: 0.303 g (91%). FAB-MS (*m*/*z*): 1245 ([M – N_2]$^+$). IR (Nujol) (cm^{-1}): 2124 (N_2) (m). ^1H NMR ($CDCl_3$) δ: 0.7–3.1 (br, C*H*$_2$, Cy of dcypb). $^{31}P\{^1H\}$ NMR ($CDCl_3$) δ: 57.5 (d, $^2J_{P,P}$ = 39 Hz), 45.0 (d, $^2J_{P,P}$ = 27 Hz), 44.6 (d, $^2J_{P,P}$ = 39 Hz), 42.3 (d, $^2J_{P,P}$ = 27 Hz); (C_6D_6) δ: 60.1 (d, $^2J_{P,P}$ = 39 Hz), 49.1 (d, $^2J_{P,P}$ = 26 Hz), 45.3 (d, $^2J_{P,P}$ = 39 Hz), 37.4 (d, $^2J_{P,P}$ = 26 Hz). Solid-state $^{31}P\{^1H\}$ CP-MAS NMR (80.9 MHz) δ: 45–57 (br, unresolved), 43.6 (br), 41.2 (br). Anal. calcd. for $C_{56}H_{104}Cl_4N_2P_4Ru_2$: C 52.81, H 8.25, N 2.20; found: C 52.90, H 8.19, N 1.90.

Preparation of $Ru_2Cl_5(dcypb)_2$ (5)

Complex **4a** (40 mg, 0.04 mmol) was dissolved in $CDCl_3$ (0.5 mL) and the solution was monitored by $^{31}P\{^1H\}$ NMR. Resolution degraded perceptibly over ~30 min, and a broad singlet emerged at 50 ppm. On further reaction, S/N values decreased, and many new peaks could be discerned (46–63, 15–32 ppm). Slow evaporation deposited red crystals of **5**.

Decomposition of 4a under vacuum

(*i*) NMR-scale. A solution of **4a** (3.0 mg, 4.7 μmol Ru) in C_6D_6, with *t*-$RuCl_2(dppe)_2$ (2.3 mg, 2.35 μmol) as an internal standard, was freeze-pump-thaw degassed in a round-bottom Schlenk flask. $^{31}P\{^1H\}$ NMR spectra were measured after every second cycle of degassing. No NMR signals were discerned after six degassing cycles, though gas evolution was sustained over three further cycles. (*ii*) Large-scale. A suspension of **4a** (20 mg, 0.016 mmol Ru_2) in benzene (10 mL) was freeze-pump-thaw degassed until no signals were evident by NMR. Concentration and addition of cold hexanes afforded a dark grey-green solid, which was filtered off, washed with cold hexanes, and dried under a flow of Ar. Yield: 16 mg. IR (Nujol) (cm^{-1}): 1944 (Ru-H) (m-w), 1629 (C=C) (m-w). (*iii*) Prolonged exposure of solid **4a** to vacuum at 50°C resulted in a mixture of diamagnetic products (multiple ^{31}P NMR signals in the region from 75 to –15 ppm).

NMR-scale preparation of $Ru_2Cl_4(dcypb)_2(H_2)$ (6)

Stirring a suspension of **4a** (4 mg, 3 μmol Ru_2) in C_6D_6 (0.5 mL) under H_2 at room temperature afforded a homogeneous orange solution within 15 min. No starting material was spectroscopically observable after 30 min. ^1H NMR (C_6D_6) δ: 0.6–3.0 (br, C*H*$_2$, Cy of dcypb), –11.8 (br s, *H*$_2$). $^{31}P\{^1H\}$ NMR (C_6D_6) δ: 65.1 (d, $^2J_{P,P}$ = 25 Hz), 59.2 (d, $^2J_{P,P}$ = 40 Hz), 45.9 (d, $^2J_{P,P}$ = 25 Hz), 43.9 (d, $^2J_{P,P}$ = 40 Hz). Hydride T_1 (min) = 26 msec (300 K, 500 MHz).

Preparation of $RuCl_2(dcypb)(CO)_2$ (ccc-(7), tcc-(8))

A suspension of **4a** (27 mg, 39 μmol Ru_2) in THF (5 mL) was stirred under CO for 24 h, affording a clear yellow solution. The solution was concentrated and hexanes added to coprecipitate **7** and **8** as a yellow powder (1:4). Yield: 23 mg (88%). IR (Nujol) (cm^{-1}): 2052 (CO) (s, **7**), 2038 (s, **8**), 1976 (s, **8**), 1962 (s, **7**). ^1H NMR (C_6D_6) δ: 0.8–2.4 (br, C*H*$_2$, Cy of dcypb). $^{13}C\{^1H\}$ NMR (C_6D_6) δ: 198.7 (t, $^2J_{P,P(cis)}$ = 12 Hz, **7**), 193.5 (dd, $^2J_{P,P(trans)}$ = 113 Hz, $^2J_{P,P(cis)}$ = 11 Hz, **7**), 193.8 (dd, $^2J_{P,P(trans)}$ = 109 Hz, $^2J_{P,P(cis)}$ = 23 Hz, **8**). $^{31}P\{^1H\}$ NMR (C_6D_6) δ: 39.4 (d, $^2J_{P,P}$ = 22 Hz, **7**), 17.1 (d, $^2J_{P,P}$ = 22 Hz, **7**), 13.8 (s, **8**). Anal. calcd. for $C_{30}H_{52}Cl_2O_2P_2Ru$: C 53.09, H 7.72; found: C 53.39, H 7.93.

In situ polymerization of norbornene by 1a

Optimization of the procedure has been described (2). Blank polymerization experiments carried out without added Ru catalyst showed no ROMP over 24 h. In a representative catalytic procedure, $PhCHN_2$ (1.1 μL, 10.6 μmol) was added to an orange suspension of **4a** (6.6 mg, 10.6 μmol) in C_6D_6 (2 mL). Vigorous bubbling ensued, and all of the solids dissolved, forming a deep orange solution, which was immediately added to a stirred solution of norbornene (200 mg, 2.1 mmol) in $CDCl_3$ or C_6D_6 (5 mL). The progress of the reaction was monitored by removing aliquots for NMR analysis. (*i*) ROMP via **4a** + 2 $PhCHN_2$ in $CDCl_3$–C_6D_6: M_n 2.4 × 10^6, M_w/M_n = 1.4; (*ii*) via **2a** (prepared in situ by addition of 2 equiv PPh_3 to **4a**) + $PhCHN_2$ in $CDCl_3$–C_6D_6: M_n 2.4 × 10^6, M_w/M_n = 1.2; (*iii*) via **4a** + 2 $PhCHN_2$ in neat benzene: bimodal, M_n 1.9 × 10^6, M_w/M_n = 2.4; M_n 20 000, M_w/M_n = 3.8.

X-ray crystallographic analysis of 5

Crystal and data collection parameters for **5** are provided in Table 1.[2] Suitable crystals were selected, mounted on thin glass fibres using viscous oil, and cooled to the data collection temperature. Data were collected on a Bruker AX SMART 1k CCD diffractometer using 0.3° ω-scans at 0, 90,

[2] Copies of materials on deposit may be purchased from The Depository of Unpublished Data, Document Delivery, CISTI, National Research Council of Canada, Ottawa, ON K1A OS2, Canada. Tables of hydrogen atom coordinates and bond lengths and angles have also been deposited with the Cambridge Crystallographic Database, and can be obtained on request from the Director, Cambridge Crystallographic Data Centre, University Chemical Laboratory, 12 Union Road, Cambridge CB2 1EZ, U.K.

Scheme 1.

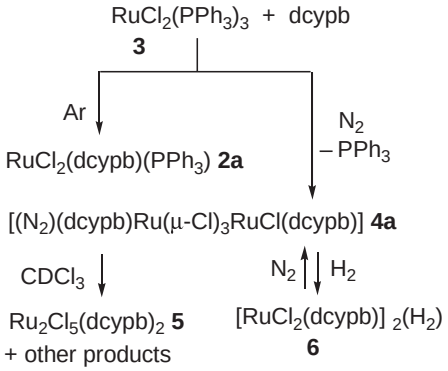

and 180° in ϕ. Unit-cell parameters were determined from 60 data frames collected at different sections of the Ewald sphere. Semi-empirical absorption corrections based on equivalent reflections were applied (9). No symmetry higher than triclinic was evident from the diffraction data. Solution in $P\bar{1}$ yielded chemically reasonable and computationally stable results of refinement. The structure was solved by direct methods, completed with difference Fourier syntheses and refined with full-matrix least-squares procedures based on F^2. A carbon atom, C(14), in one of the ligands was located conformationally disordered in two positions with roughly 50/50 site occupation distribution. The large anisotropic displacement parameters on C(13) suggest similar disorder. Attempts to model this disorder were unsuccessful, however, owing to insufficient resolution between the contributing atomic positions. A molecule of benzene and two molecules of chloroform were located in the asymmetric unit. The benzene molecule of crystallization was constrained as flat hexagon. All nonhydrogen atoms were refined with anisotropic displacement parameters. All hydrogen atoms were treated as idealized contributions. All scattering factors and anomalous dispersion factors are contained in the SHEXTL 5.10 program library (10).

Results and discussion

Treatment of **3** with dcypb in benzene under Ar yields the mixed-phosphine complex **2a** (11), which differs from its dppb analogue **2b** in undergoing no dimerization (with loss of PPh_3) in solution. The very high solubility of **2a** has so far prevented its isolation. In strong contrast is the reaction of **3** with dcypb under N_2 atmosphere, which affords a high-yield route to sparingly soluble $[(N_2)Ru(dcypb)(\mu\text{-}Cl)_3RuCl(dcypb)]$ (**4a**) (Scheme 1). This net displacement of triphenylphosphine ligand by N_2 has no precedent in the corresponding aryldiphosphine chemistry. The identity of **4a** is confirmed by NMR and IR spectroscopy and microanalysis. ^{31}P NMR analysis reveals four doublets for the inequivalent phosphine groups within **4a**, in a pattern similar to that earlier reported (12) for dppb analogue **4b**. The ^1H NMR spectrum of **4a** is less informative, consisting only of a series of overlapping multiplets between 0.7–3.1 ppm arising from the cyclohexyl protons and the methylene protons of the dcypb backbone. A strong IR band for ν(N≡N) is evident at 2124 cm^{-1}.

Fig. 1. ORTEP drawing of $Ru_2Cl_5(dcypb)_2$ (**5**). Thermal ellipsoids depicted at 30% probability level; cyclohexyl rings, hydrogen atoms, and solvate molecules omitted for clarity. A detailed structural representation is included in the Supplementary Material.

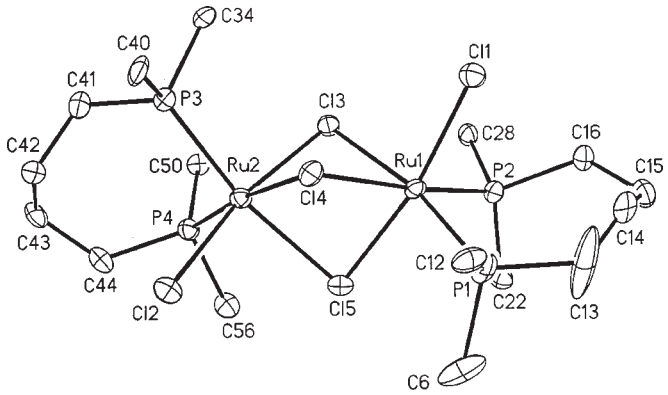

The solubility of **4a** is slightly improved in halogenated solvents such as CH_2Cl_2 or $CDCl_3$, but decomposition in these solvents yields the mixed-valence dimer $Ru_2Cl_5(dcypb)_2$ **5**.[3] James and co-workers (12, 13) have reported extensively on the synthesis, reactivity, and catalytic chemistry of such species, obtained via reaction of chelating diphosphines with $RuCl_3(PR_3)_2$ (R = Ph, *p*-tolyl). Attempts to prepare clean **5** on large scale by the reaction of **4a** with $CDCl_3$ or ethereal HCl, resulted in product mixtures, as judged by in situ ^{31}P NMR analysis prior to complete loss of the diamagnetic signals. Slow evaporation of $CDCl_3$ solutions under N_2 permitted isolation of crystals suitable for X-ray analysis. The molecular structure of **5** is shown in Fig. 1; crystal data and selected structural parameters appear in Tables 1 and 2, respectively.

Complex **5** adopts a triply chloride-bridged diruthenium structure, in which the coordination geometry at each metal center is distorted octahedral. The structure is unsymmetrical, with one of the octahedra being rotated by 120° about the Ru–Ru vector. A similar structure was earlier reported for $Ru_2Cl_5(P(n\text{-}Bu)_3)_4$ (14), whereas the only previous crystal structure of a chelating diphosphine derivative, $Ru_2Cl_5(chiraphos)_2$, exhibits a symmetrical ligand arrangement (13). Ruthenium—phosphorus and —chloride distances fall within the ranges reported, as do angles within the Ru-P-Cl skeleton. Chloride atoms *trans* to phosphorus display distinctly longer Ru—Cl bond distances (av. 2.49 Å) compared to those *trans* to Cl (av. 2.38 Å), as expected from the stronger *trans* influence of phosphine. The average bridging angle in **5** (83.7°) is nearly 15° larger than the ideal value of 70.5° for two regular face-sharing octahedra (14), indicating that the Ru centers are further apart than expected for a regular cofacial bioctahedron. The Ru—Ru distance of 3.278 Å is considerably longer than the upper limit associated with the presence of a metal–metal bond (2.95 Å) (13). As with the chiraphos and the $P(n\text{-}Bu)_3$ complexes, the crystallographic data do not permit assignment of formal oxidation states to the ruthenium atoms.

[3] Note added in proof: complex **5** was originally prepared via this route, and partially transformed into **6** by treatment with H_2 in DMA or CH_2Cl_2. Private communication from B.R. James, based on data contained in ref. 6.

Table 1. Crystal data and structure refinement for **5**.

Empirical formula	$C_{64}H_{112}Cl_{11}P_4Ru_2$
FW	1597.51
T (K)	203(2)
Wavelength (Å)	0.71073
Crystal system, space group	Triclinic, $P\bar{1}$
Unit cell dimensions	
a, b, c (Å)	13.390(2), 15.726(2), 19.524(2)
α, β, γ (°)	77.325(2), 70.964(2), 73.478(2)
Volume (Å^3)	3689.3(8)
Z, density$_{calcd.}$ (mg m^{-3})	2, 1.438
Absorption coefficient (mm^{-1})	0.932
F(000)	1662
Crystal size (mm)	0.10 × 0.10 × 0.03
Theta range for data collection (°)	1.11–20.81
Limiting indices	$-12 \le h \le 13$, $-15 \le k \le 15$, $0 \le l \le 19$
Reflections collected/unique ($R_{(int)}$ = 0.1237)	29133/7712
Completeness to θ = 28.83	99.7
Absorption correction	Semi-empirical from equivalents
Max. and min. transmission	0.928077 and 0.637019
Refinement method on F^2	Full-matrix least-squares
Data/restraints/parameters	7712/0/722
GoF on F^2	1.025
R^a	0.0533
$R_w{}^b$	0.1009

[a] $R = \Sigma||F_o| - |F_c||/\Sigma|F_o|$.
[b] $R_w = [\Sigma w\delta^2/\Sigma wF_o{}^2]^{1/2}$.

Table 2. Selected bond lengths (Å) and angles (°) for (**5**).

Bond lengths (Å)			
Ru(1)—P(1)	2.309(3)	Ru(2)—P(3)	2.323(2)
Ru(1)—P(2)	2.325(3)	Ru(2)—P(4)	2.348(3)
Ru(1)—Cl(5)	2.395(2)	Ru(2)—Cl(2)	2.360(3)
Ru(1)—Cl(1)	2.387(2)	Ru(2)—Cl(3)	2.373(2)
Ru(1)—Cl(3)	2.495(2)	Ru(2)—Cl(4)	2.466(2)
Ru(1)—Cl(4)	2.504(2)	Ru(2)—Cl(5)	2.505(2)
Bond angles (°)			
P(1)-Ru(1)-P(2)	95.14(9)	P(3)-Ru(2)-P(4)	93.75(9)
Cl(5)-Ru(1)-Cl(1)	168.81(8)	Cl(2)-Ru(2)-Cl(3)	168.58(9)
P(1)-Ru(1)-Cl(3)	169.32(9)	P(3)-Ru(2)-Cl(5)	168.60(9)
P(2)-Ru(1)-Cl(4)	172.19(9)	P(4)-Ru(2)-Cl(4)	173.97(9)

In aromatic solvents, **4a** is stable for weeks in solution under N_2. In contrast with the dppb systems, which exist in equilibrium with the "naked" dimers $[RuCl_2(PP)]_2$ **9** under N_2 (eq. [1], (12)), no peaks for $[RuCl_2(dcypb)]_2$ are observed.

[1] $$\underset{\mathbf{4}}{Ru_2Cl_4(PP)_2(N_2)} \rightleftharpoons \underset{\mathbf{9}}{Ru_2Cl_4(PP)_2} + N_2$$

The lability of the dinitrogen ligand is indicated, however, by its facile replacement under H_2 or CO atmosphere. Displacement of N_2 by dihydrogen is complete within 10 min at 1 atm H_2, as indicated by a pronounced shift in the location of the ^{31}P NMR doublets associated with the "L-end" of the complex (Table 3). The ^1H NMR spectrum reveals a singlet for bound H_2 at –11.8 ppm. The T_1 (min) value of 26 msec (300 K, 500 MHz) corresponds to an H—H distance of 0.89 Å, assuming rapid rotation of the dihydrogen ligand; this compares well with the value of 0.86 Å reported for **4b** (15). H_2-coordination is readily reversed under N_2 atmosphere. Under CO, mononuclear $RuCl_2(dcypb)(CO)_2$ is formed as a mixture of isomers, **7** and **8** (Scheme 2). The two are readily distinguished by $^{31}P\{^1H\}$ NMR; the phosphine groups of *all-cis*-**7** appear as a pair of doublets, whereas a singlet is found for *tcc*-**8**. Consistent with the proposed structures is the carbonyl region of the $^{13}C\{^1H\}$ NMR spectrum, as well as the IR data. The former shows a triplet and a doublet of doublets for **7**, but only a doublet of doublets for **8**. Two IR ν(CO) bands are seen for each complex.

Surprisingly, in view of the observed lability of the dinitrogen ligand in **4a**, no peaks for a dimer of type **9** were evident even under Ar atmosphere, or following freeze-pump-thaw (FPT) experiments carried out to shift the presumed equilibrium (eq. [1]) to the right. Sustained gas evolution was observed in NMR tubes subjected to successive FPT cycles (>20), but no new peaks were evident by $^{31}P\{^1H\}$ NMR, even at low temperature (183 K). Degassing experiments using *trans*-$RuCl_2(dppe)_2$ as internal standard were carried out in Schlenk vessels, in which the higher surface area permitted more efficient removal of dissolved gas. A steady decrease in concentration of **4a** is measured with increasing number of FPT cycles, signifying conversion of **4a** to a paramagnetic Ru product. Gas evolution is sustained after complete loss of the NMR signals, probably owing to paramagnetic broadening of signals for remaining **4a**. Observation of a large ^1H NMR singlet for dissolved H_2 at 4.2 ppm after each FPT cycle is consistent with Ru-promoted

Table 3. $^{31}P\{^{1}H\}$ NMR data for $Ru_2Cl_4(PP)_2(L)$ complexes.

Complex	Chemical shifts (δ, ppm)	$^{2}J_{P,P}$ (Hz)
$Ru_2Cl_4(dcypb)_2(N_2)$ (**4a**)	60.1 (d), 45.3 (d); 49.1 (d), 37.4 (d)	40; 26
$Ru_2Cl_4(dppb)_2(N_2)$ (**4b**) (12)	54.4 (d), 53.5 (d); 46.6 (d), 36.8 (d)	45; 32
$Ru_2Cl_4(dcypb)_2(H_2)$ (**6**)	59.2 (d), 43.9 (d); 65.1 (d), 45.9 (d)	40; 25

Note: Measured at room temperature in C_6D_6, 121 MHz.

Scheme 2.

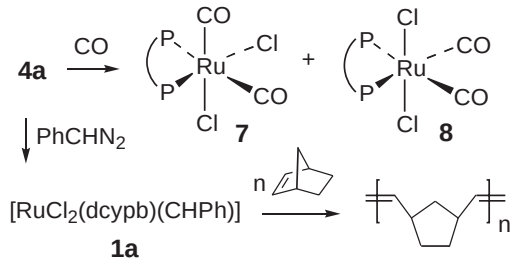

dehydrogenation of the cyclohexyl rings and (or) the dcypb backbone (catalytic dehydrogenation of the solvent itself is excluded by observation of this behaviour in benzene solvent). A ν(C=C) stretching band appears at 1629 cm^{-1} in the IR spectrum, as well as a signal at 1944 cm^{-1} assigned to Ru–H. No HCl was detected by GC-MS, and no precipitate formed on forcing the effluent gas through concentrated ammonia or NH_4PF_6 solutions, suggesting that HCl is not evolved in the reaction.

The utility of closely related Ru complexes in catalytic dehydrogenation of sp^3 C–H bonds has been established by Leitner and co-workers (16, 17). While forcing conditions were required for activation of cyclooctane, dehydrogenation of the cyclohexyl rings within complexes containing $Cy_2P(CH_2)_nPCy_2$ (n = 3, 4) was induced at 50°C, resulting in diamagnetic η^3-cyclohexenyl derivatives. Chaudret and co-workers (18–20) have likewise described intramolecular dehydrogenation of cyclohexyl rings within Ru–PCy_3 complexes at room temperature, affording Ru(II) complexes containing η^3- and (or) η^2-cyclohexenyl rings. A related process is almost certainly involved in dehydrogenation of **4a**, in which retention of both chloride ligands may be responsible for formation of a Ru(III) product. We do not exclude the possibility of concomitant attack on the four-carbon backbone; agostic interactions between Ru and bound dppb, culminating in deuterium incorporation into the backbone methylene groups, have been noted (21), while we have observed C–H bond activation within the dcypb backbone in related silylene chemistry (22). Confirmation of the identity of the dehydrogenation product(s) is hampered by paramagnetism and poor crystallinity. Attempts to probe the reaction by thermal gravimetric analysis are complicated by the observation of other diamagnetic products in solid-state degassing experiments. The high activity of these species toward activation of saturated C–H bonds under exceptionally mild conditions is notable; however, facile intramolecular attack may be attributed to the combination of steric bulk and high basicity in the dcypb ligand. The ease of such reactions in the absence of stabilizing donor ligands may account for prior difficulties in gaining access to this chemistry under Ar atmosphere. Use of N_2 as a labile donor to inhibit intramolecular attack opens up a potentially rich catalytic and coordination chemistry.

Fig. 2. ROMP activity of dcypb complexes. (*a*) **4a** + 2 $PhCHN_2$, $CDCl_3$-C_6D_6; (*b*) **2a** + 2 $PhCHN_2$, $CDCl_3$-C_6D_6; and (*c*) **4a** + 2 $PhCHN_2$, C_6D_6.

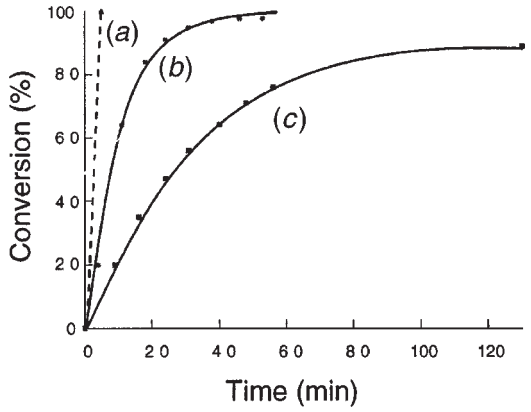

We recently described polymerization via $RuCl_2(PP)(CHPh)$ systems derived from **2**, in which high ROMP activity in norbornene polymerization was observed despite the presence of the catalyst poison PPh_3 (2). PPh_3-free **1a**, generated in situ by addition of $PhCHN_2$ to **4a** (Scheme 2), functions as a much more avid catalyst (Fig. 2). Thus, while ROMP of norbornene by the **2a**–$PhCHN_2$ system requires nearly an hour at substrate:catalyst ratios of 200:1, polymerization via **4a** is complete before the first NMR measurement can be taken (5 min, lower limit for the turnover frequency = 2400 h^{-1}). Despite the susceptibility of **4a** to decomposition by chlorinated solvent, mixed solvent systems, in which the catalyst was generated in C_6D_6 and subsequently added to a $CDCl_3$ solution of norbornene, showed much higher activity than ROMP in neat C_6D_6. Decreased metathesis activity in nonpolar solvents is characteristic of these Ru systems (1). The slow rate of polymerization in neat benzene permits competing decomposition via extrusion of the carbene as stilbene (a process characteristic of Ru–carbene complexes). Polymer polydispersities for reactions in benzene are consequently *higher* than those observed in the mixed solvent systems (PDI 3.8 vs. 1.2–1.4), and a bimodal molecular weight distribution is observed, indicating the presence of more than one ROMP-active species. The very rapid rate of polymerization in $CDCl_3$–C_6D_6 (Fig. 2*a*) suggests that decomposition of **1a** cannot compete with norbornene metathesis in this solvent system, and this is supported by the low polydispersity obtained.

Conclusions

The foregoing describes the first general route into the chemistry of chlororuthenium–phosphine complexes con-

taining the basic, bulky diphosphine, dcypb. Steric pressure, allied with high electron density, renders these species susceptible to decomposition by attack on solvent or on the dcypb ligands. Where such processes can be restrained, this heightened reactivity can be redirected and exploited in catalysis, as exemplified in the potent ROMP reactivity of the carbene derivative.

Acknowledgments

This work was supported by the Natural Sciences and Engineering Research Council of Canada (NSERC), the Canada Foundation for Innovation, and the Ontario Innovation Trust.

References

1. (*a*) E.L. Dias, S.T. Nguyen, and R.H. Grubbs. J. Am. Chem. Soc. **119**, 3887 (1997); (*b*) P. Schwab, R.H. Grubbs, and J.W. Ziller. J. Am. Chem. Soc. **118**, 100 (1996).
2. D. Amoroso and D.E. Fogg. Macromolecules, **33**, 2815 (2000).
3. M. Burk, J.P. Martinez, J.E. Feaster, and N. Cosford. Tetrahedron, **50**, 4399 (1994).
4. N.T. McManus and G.L. Rempel. J. Macromol. Sci. R. M. C. **C35**, 239 (1995).
5. X. Creary. *In* Organic syntheses. Vol. VII. *Edited by* J. P. Freeman. John Wiley & Sons, Toronto. 1990. p. 438.
6. D.E.K.Y. Chau. M.Sc. thesis. University of British Columbia. Vancouver, B.C. 1992.
7. P.S. Hallman, T.A. Stephenson, and G. Wilkinson. Inorg. Synth. **12**, 237 (1970).
8. J. Chatt and R.G. Hayter. J. Chem. Soc. 896 (1961).
9. R. Blessing. Acta Crystallogr. Sect. A: Fundam. Crystallogr. **A51**, 33 (1995).
10. G.M. Sheldrick. Bruker AXS, Madison, WI. 1997.
11. K.S. MacFarlane, A.M. Joshi, S.J. Rettig, and B.R. James. Inorg. Chem. **35**, 7304 (1996).
12. A.M. Joshi, I.S. Thorburn, S.J. Rettig, and B.R. James. Inorg. Chim. Acta, **198**–**200**, 283 (1992).
13. I.S. Thorburn, S.J. Rettig, and B.R. James. Inorg. Chem. **25**, 234 (1986), and refs. cited therein.
14. G. Chioccala and J.J. Daly. J. Chem. Soc. A. 1981 (1968).
15. A.M. Joshi and B.R. James. J. Chem. Soc. Chem. Commun. 1785 (1989).
16. C. Six, B. Gabor, H. Gorls, R. Mynott, P. Philipps, and W. Leitner. Organometallics, **18**, 3316 (1999).
17. W. Leitner and C. Six. Chem. Ber. **130**, 555 (1997).
18. S. Sabo-Etienne and B. Chaudret. Coord. Chem. Rev. **178**–**180**, 381 (1998).
19. B. Chaudret, P. Dagnac, D. Labroue, and S. Sabo-Etienne. New J. Chem. **20**, 1137 (1996).
20. M.L. Christ, S. Sabo-Etienne, and B. Chaudret. Organometallics, **14**, 1082 (1995).
21. M. Ogasawara and M. Saburi. Organometallics, **13**, 1911 (1994).
22. D. Amoroso, M. Haaf, G.P.A. Yap, R. West, and D.E. Fogg. Organometallics, accepted.